EUROPHYSICS LETTERS 15 March 2004

Europhys. Lett., **65** (6), pp. 753–759 (2004)
DOI: 10.1209/epl/i2003-10132-1

Self-organized criticality in the Bean state in $YBa_2Cu_3O_{7-x}$ thin films

C. M. Aegerter, M. S. Welling and R. J. Wijngaarden

Division of Physics and Astronomy, Vrije Universiteit
De Boelelaan 1081, 1081HV Amsterdam, The Netherlands

(received 4 August 2003; accepted in final form 22 January 2004)

PACS. 05.65.+b – Self-organized systems.
PACS. 45.70.Vn – Granular models of complex systems; traffic flow.
PACS. 74.25.Qt – Vortex lattices, flux pinning, flux creep.

Abstract. – The penetration of magnetic flux into a thin film of $YBa_2Cu_3O_{7-x}$ is studied when the external field is ramped slowly. In this case, the flux penetrates in bursts or avalanches. The size of these avalanches is distributed according to a power law with an exponent of $\tau = 1.29(2)$. The additional observation of finite-size scaling of the avalanche distributions, with an avalanche dimension $D = 1.89(3)$, gives strong indications towards self-organized criticality in this system. Furthermore, we determine exponents governing the roughening dynamics of the flux surface using some universal scaling relations. These exponents are compared to those obtained from a standard roughening analysis.

The critical state in a type-II superconductor shows a powerful analogy to a granular pile, which was already noted by de Gennes in the 1960s [1]. With the advent of self-organized criticality (SOC) [2], the avalanche behavior of granular piles was intensely studied [3,4]. This is because SOC was thought of as a general mechanism to explain the intermittent behavior of slowly driven systems far from thermodynamic equilibrium. The experimental verification of SOC, however, was not straightforward. Power law distribution of avalanches was not observed in many experiments [5, 6]. One of the hallmarks of critical behavior, finite-size scaling, was only found in a few cases, most notably in experiments on a one-dimensional (1d) pile of rice [7], as well as in a 1d pile of steel balls with a random distribution of balls in the bottom layer [8]. The only studies of finite-size scaling in a 2d system to date are, to our knowledge, a study by some of us on the properties of a 2d pile of rice [9], which is qualitatively similar to the one presented here, and a study of a conical pile of beads [10] again with similar results.

Given the classical analogy with granular piles [11], the critical state in superconductors was also quickly proposed as a SOC system [12]. Experimentally, magnetic vortices are well suited to study SOC, since kinetic effects, which can lead to deviations from critical behavior in sand piles [7, 13], are naturally suppressed due to their overdamped dynamics [14]. Just as in the case of granular piles, however, the experimental confirmation of this conjecture has been controversial. While power law behavior in the avalanche distribution has been

© EDP Sciences

observed by most authors [15, 16], finite-size scaling was not observed so far in the case of the critical state in superconductors. This is because most of the studies [15, 17] were carried out using magnetization measurements, which only give information on the overall behavior of the whole of the sample. This corresponds to only considering off-edge avalanches in a sand pile, which do not capture the full dynamics and may therefore give a flawed picture [13]. This is exemplified in the study of Bretz *et al.* [4], who also studies internal avalanches as we do here and did find power law behavior in a sand pile. More recent investigations using arrays of miniature Hall probes [16], do give insights into internal avalanches and the complete dynamics, but only give information from a few selected points in the sample, which makes testing for finite-size scaling impossible.

In this letter, we study the local changes in the magnetic flux over the whole central area of a sample. This is done via a highly sensitive magneto-optic setup, which can resolve flux densities of 0.2 mT over an area of $\sim 5 \times 5\,\mu\mathrm{m}^2$. This implies that flux changes corresponding to 2.5 Φ_0 can be resolved, where $\Phi_0 = h/2e$ is the magnetic-flux quantum (the flux of a single vortex). Furthermore, since we observe a large field of view, different size subsets can be studied leading to the possibility of observing finite-size scaling. Given the finite-size scaling exponents, one can determine the roughening and dynamical exponents of the flux-surface from universal scaling relations. Comparing these results with those determined directly from the surface properties [18] gives good agreement.

The experiments were carried out on a thin film of $YBa_2Cu_3O_{7-x}$ (YBCO), grown on a $NdGaO_3$ substrate to a thickness of 80 nm using pulsed-laser ablation [19]. The pinning sites in the sample are uniformly distributed and consist mostly of screw dislocations acting as point pins [20]. A polarization microscope was placed in an Oxford Instruments cryomagnet capable of a maximum field of 1 T and cooling to a temperature of 1.8 K. The sample was cooled in zero field to 4.2 K, at which point the external field was slowly increased in steps of $\mu_0 \Delta H = 50\,\mu\mathrm{T}$, after which the sample was allowed to relax for 10 s before an image was taken. In a magneto-optical experiment, the flux density $B_z(x, y)$ at the surface of the sample is measured via an indicator layer showing a strong Faraday effect. The polarization of the incoming light is turned in proportion to the flux density in the indicator layer. A cross-polarized analyzer will thus admit light from regions with non-zero magnetic-flux density [21]. However, in order to determine the rotation angle (and thus the flux density B_z) directly, including its sign, we employ a recently developed magneto-optic image lock-in amplifier [22], using a modulation of the incoming polarization vector. The output of the instrument gives directly the Faraday angle for each pixel, independent of spatial inhomogeneities in the illumination.

The data analyzed here come from a series of nine experimental runs, each consisting of $\sim$ 300 time steps. Of these steps only the last 140 in each run were used, in order to have a critical state established in the whole region of the sample used for analysis. The size and shape of the avalanches was determined from the difference $\Delta B_z(x, y)$ of two consecutive images (see fig. 1). From this difference, the average increase in the applied magnetic field, due to the step-wise field sweep, was subtracted in order to solely study the avalanches. The external fields were determined from a region well outside the sample, which was also in the field of view. Once the incremental field difference is determined, the size of an avalanche, corresponding to the displaced amount of flux $\Delta\Phi$, is obtained from ΔB_z via integration over the whole area:

$$s = \Delta\Phi = \frac{1}{2} \int |\Delta B_z(x, y)| \mathrm{d}x\, \mathrm{d}y. \tag{1}$$

The average increase in the external field is in good agreement with the increase in flux density of $50\,\mu\mathrm{T}$ between images. The resulting time series of the avalanche behavior of all the experiments is shown in fig. 2. In this figure, ΔB_z was integrated over the whole area of

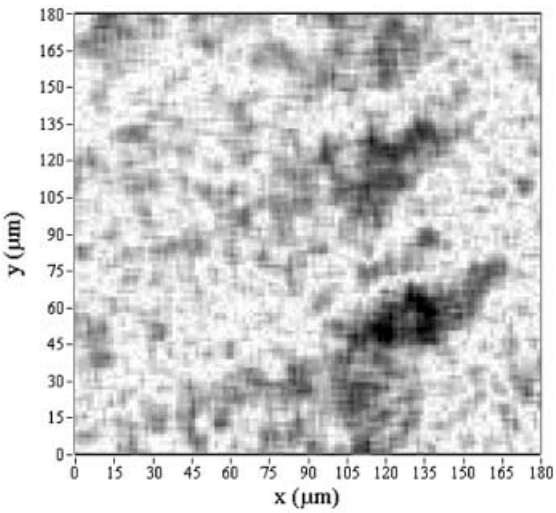

Fig. 1 – Snapshot of a flux avalanche. Shown is the difference between two consecutive field profiles $\Delta B_z(x, y)$. The scale goes from 0 (white) to 0.4 mT (black). The area-integral over this difference corresponds to the size of the flux jump $\Delta\Phi$. In order to determine the roughness exponent of the whole surface, we also need to determine the fractal dimension of the active sites in such an avalanche (see text).

$180 \times 180\,\mu\text{m}^2$ in each time step. As can be seen, the evolution of the magnetic flux inside the sample is intermittent with occasional large jumps.

In order to check the data for finite-size scaling, we also integrated ΔB_z over subsets of the image of a linear size of $L = 90$, 45 and $15\,\mu$m, respectively. The histograms of the avalanche size distribution for these data-sets are shown unscaled in fig. 3a. As can be seen, the smallest avalanches correspond to a flux change of 2-3 Φ_0, corresponding to the resolution of the measurement. Taking all of the data together, we observe a power law distribution over more than three decades. The slope of the black line gives the exponent of the distribution,

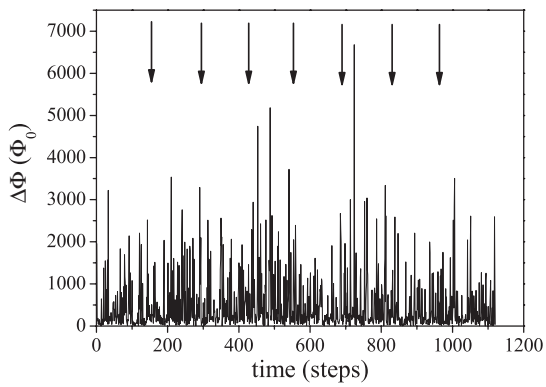

Fig. 2 – The time evolution of the magnetic flux inside the sample over all nine experiments. The magnetic-field difference ΔB_z has been integrated over the whole surface of $180 \times 180\,\mu\text{m}^2$ and the average flux increase has been subtracted. The evolution takes place in the form of flux jumps or avalanches of various sizes, which are summarized in the histogram of fig. 3. The different experimental runs are separated by arrows.

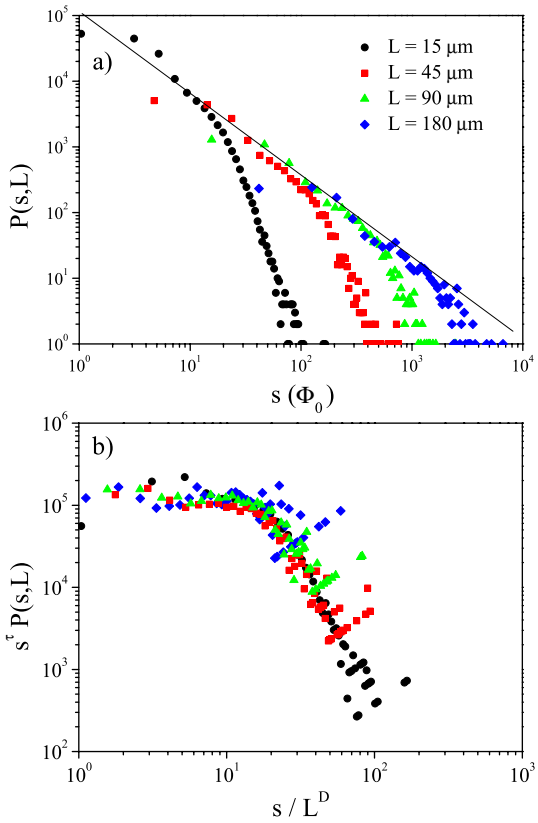

Fig. 3 – (a) The direct avalanche size distribution for different sizes of windows (180, 90, 45, and 15 μm, respectively). There is an envelope to the distribution in the form of a power law indicated by the black line over more than three decades with an exponent of $\tau = 1.30(5)$. (b) The scaled size distributions showing a curve collapse. The exponents used in the finite-size scaling are $\tau = 1.29(2)$ and $D = 1.89(3)$.

$\tau = 1.30(5)$. In fig. 3b we show the same data, but now the probabilities are scaled with s^τ and the avalanche sizes are scaled with L^{-D}. As can be seen, there is very good curve collapse indicating the presence of finite-size scaling [23]. This means that the avalanche size distribution function is given by

$$P(s, L) = s^{-\tau} f\left(\frac{s}{L^D}\right), \tag{2}$$

where $f(x)$ is constant up to a cut-off scale $s_{\mathrm{co}} \propto L^D$. The values of the exponents used to obtain curve collapse are $\tau = 1.29(2)$ and $D = 1.89(3)$. Note that, here, we have carried out the finite-size scaling by way of subdividing the whole image rather than carrying out experiments with different size samples. We have checked by means of simulations of the 2d Oslo-model that such a subdivision into finite-size samples leads to the same scaling exponents as a curve collapse of different simulations of finite size. Furthermore, an independent measurement of D, directly using a box-counting method [24] in 3d yields $D = 1.92(5)$, consistent with the value from finite-size scaling.

Note also that molecular-dynamics simulations of the movement of vortices by Olson *et al.* [27] observe power-law–distributed avalanches as well. For a range of pinning strengths,

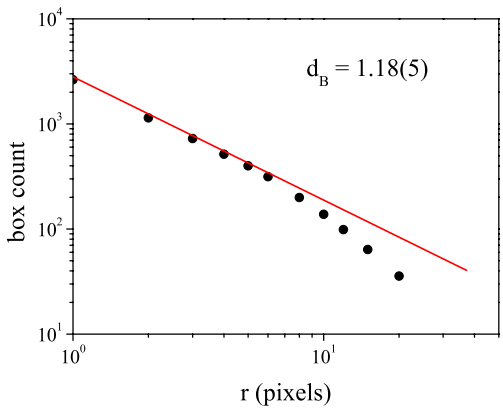

Fig. 4 – Determination of the fractal dimension of the active clusters in an avalanche using the box-counting method. In this determination, avalanches more than one standard deviation larger than the average size have been used. The analysis of one such cluster is shown. The fractal dimension is given by the slope of the straight line. Averaged over all clusters, this leads to a fractal dimension of the active clusters of $d_B = 1.18(5)$.

the exponents obtained in that work are between $1 < \tau < 1.4$, in reasonable agreement with the value found here.

It has already been noted [25] that the front of penetrating flux shows kinetic roughening. Similarly, the surface $B_z(x, y)$ in two dimensions can be shown to be self-affine, with a roughness exponent α, characterizing the growth of the interface width w_{sat} with the system size, $w_{\text{sat}} \propto L^{\alpha}$ and a dynamic exponent z characterizing the saturation time of the width. In such an analysis of the present data, discussed elsewhere [18], the roughness exponent was found to be $\alpha = 0.73(5)$ and the dynamic exponent was found to be $z = 1.38(10)$. Using the universal scaling relations derived by Paczuski *et al.* [26] for various SOC models, these exponents characterizing the roughness and growth of the surface can also be determined from the scaling exponents of the avalanche distribution. This indicates that the roughening of the surface originates from the avalanche distribution and its underlying dynamics.

Let us first discuss the roughness exponent. According to the finite-size scaling, an avalanche of the cut-off size will scale like $s_{\text{co}} \propto L^D$. Similarly, the size of such an avalanche will roughly be given by $s_{\text{co}} \simeq w_{\text{sat}} L^{d_B}$, where d_B is the fractal dimension of the area of an avalanche. Equating the two expressions for s_{co}, one obtains $w_{\text{sat}} \propto L^{D-d_B}$ and hence

$$\alpha = D - d_B, \tag{3}$$

in agreement with ref. [26]. In order to determine the roughness exponent from the avalanches, we therefore have to measure the fractal dimension, d_B, of the avalanche's area, which was done using a simple box-counting method [24]. To this end, avalanches which were one standard deviation bigger than average were binarized, yielding a distribution of active clusters used in the determination of the fractal dimension. The result for one such cluster can be seen in fig. 4, where the number of active pixels of the avalanche is shown as a function of the length scale. Averaged over all clusters analyzed, the fractal dimension, given by the slope of the line in fig. 4, is $d_B = 1.18(5)$. From this we determine the roughness exponent as $\alpha = 0.71(5)$, in good agreement with that determined from a roughness analysis (via the correlation function and the power spectrum) of the surface fluctuations [18].

The dynamic exponent, z, can be obtained from a similar argument. The scaling of the crossover time with the system size is described by z, $t_{\times} \propto L^z$. This crossover time can be

roughly estimated from the time it takes for an avalanche of the cut-off size $s_{\rm co}$ to appear. Since flux is added to the system in constant steps, $\delta\Phi$, the number of vortices added until a cut-off avalanche occurs is given by $\delta\Phi t_\times$. On the other hand, the flux added will also be moved in smaller avalanches. The total flux necessary to be introduced in order to obtain an avalanche of size $s_{\rm co}$ can be estimated from integrating over all avalanche sizes up to the one of size $s_{\rm co}$:

$$t_\times \propto \int_0^{s_{\rm co}} sP(s)\mathrm{d}s \propto s_{\rm co}^{2-\tau}. \tag{4}$$

Using $s_{\rm co} \propto L^D$, we obtain $t_\times \propto L^{D(2-\tau)}$, which immediately leads to the scaling relation

$$z = D(2-\tau). \tag{5}$$

Again, this is also in agreement with the universal scaling relation derived by Paczuski *et al.* [26]. Inserting the values determined above, we obtain $z = 1.34(4)$, again in good agreement with that determined via a roughness analysis [18].

In conclusion, we have shown that the distribution of the size of flux jumps in an YBCO thin film is not only given by a power law, but also shows finite-size scaling. Due to universal scaling relations valid for a SOC state [26], the exponents determined via finite-size scaling can also be used to describe other properties of the system. One such example is the roughening of the magnetic-flux surface. Here the statistical properties of the self-affine structure, built up by the penetrating flux, such as the roughness and dynamical exponent, can be derived from the structure and dynamics of the flux avalanches using relations (3) and (5). These characteristic exponents can however also be determined directly, via a roughness analysis [18], the results of which can be compared to those obtained via the avalanche dynamics. As discussed above, we find excellent agreement between the exponents determined in these separate ways. The critical state observed in the YBCO thin films can be seen as a realization of a 2d roughening system, albeit with a self-organized dynamics.

In the future, magnetic-flux structures in superconductors, as the ones studied here, may be used as an ideal experimental system with which to study non-equilibrium phenomena, especially those of granular matter. In fact we find strong qualitative correspondence of the behavior of the vortices with that of a pile of rice [9] in terms of SOC behavior. However, in addition to the granular system, the superconducting system studied here allows for the presence and control of quenched noise due to pinning sites, whose influence on the statistical properties can then be studied experimentally as well. Moreover, the physics of the microscopic behavior of vortices is well studied [14, 27], so that collective effects can be studied directly.

* * *

We would like to thank J. Rector for the growth of the samples. This work was supported by FOM (Stichting voor Fundamenteel Onderzoek der Materie), which is financially supported by NWO (Nederlandse Organisatie voor Wetenschappelijk Onderzoek).

REFERENCES

[1] de Gennes P. G., *Superconductivity of Metals and Alloys* (Addison-Wesley, New York) 1966.
[2] Bak P., Tang C. and Wiesenfeld K., *Phys. Rev. Lett.*, **59** (1987) 381; *Phys. Rev. A*, **38** (1988) 364.
[3] See, *e.g.*, Jaeger H. M., Liu C.-H. and Nagel S. R., *Phys. Rev. Lett.*, **62** (1989) 40; Rosendahl J., Vekic M. and Rutledge J. E., *Phys. Rev. Lett.*, **73** (1994) 537; Held G. A. *et al.*, *Phys. Rev. Lett.*, **65** (1990) 1120.

[4] Bretz M. *et al.*, *Phys. Rev. Lett.*, **69** (1992) 2431.
[5] Jaeger H. M., Nagel S. R. and Behringer R. P., *Rev. Mod. Phys.*, **68** (1996) 1259; Nagel S. R., *Rev. Mod. Phys.*, **64** (1992) 321 and references therein.
[6] For a review see Jensen H.-J., *Self-Organized Criticality: Emergent Complex Behavior in Physical and Biological Systems* (Cambridge University Press) 2000.
[7] Frette V. *et al.*, *Nature (London)*, **379** (1996) 49.
[8] Altshuler E. *et al.*, *Phys. Rev. Lett.*, **86** (2001) 5490.
[9] Aegerter C. M., Günther R. and Wijngaarden R. J., *Phys. Rev. E*, **67** (2003) 051306.
[10] Costello R. M. *et al.*, *Phys. Rev. E*, **67** (2003) 041304.
[11] Campbell A. M. and Evetts J. E., *Adv. Phys.*, **21** (1972) 199; Altshuler E., in *Some Contemporary Problems of Condensed Matter Physics in Contemporary Fundamental Physics*, edited by Vlaev S. J., Gaggero L. M. and Dvoeglazov V. V. (Nova Science Publishers) 2001.
[12] Zaitsev S. I., *Physica A*, **151** (1992) 411.
[13] Feder J., *Fractals* (Plenum, New York) 1989.
[14] Blatter G. *et al.*, *Rev. Mod. Phys.*, **66** (1995) 1125.
[15] Field S., Witt J. and Nori F., *Phys. Rev. Lett.*, **74** (1995) 1206; Aegerter C. M., *Phys. Rev. E*, **58** (1998) 1438.
[16] Behnia K. *et al.*, *Phys. Rev. B*, **61** (2000) R3815; *J. Magn. & Magn. Mater.*, **226** (2001) 370; Altshuler E. *et al.*, cond-mat/0208266.
[17] See, *e.g.*, Zieve R. J. *et al.*, *Phys. Rev. B*, **53** (1996) 11849; Nowak E. R. *et al.*, *Phys. Rev. B*, **55** (1997) 11702.
[18] Welling M. S., Aegerter C. M. and Wijngaarden R. J., to be published.
[19] Dam B. *et al.*, *Appl. Phys. Lett.*, **65** (1994) 1581.
[20] Dam B. *et al.*, *Nature (London)*, **399** (1999) 439.
[21] Huebener R. P., *Magnetic Flux Structures in Superconductors*, 2nd edition (Springer) 2000; Koblischka M. R. and Wijngaarden R. J., *Supercond. Sci. Technol.*, **8** (1995) 199.
[22] Wijngaarden R. J. *et al.*, *Rev. Sci. Instrum.*, **72** (2001) 2661.
[23] See, *e.g.*, Barabasi A.-L. and Stanley H. E., *Fractal Concepts in Surface Growth* (Cambridge University Press) 1995.
[24] Mandelbrot B. B., *The Fractal Geometry of Nature* (Freeman, New York) 1983.
[25] Surdeanu R. *et al.*, *Phys. Rev. Lett.*, **83** (1999) 2054.
[26] Paczuski M., Maslov S. and Bak P., *Phys. Rev. E*, **53** (1996) 414; Paczuski M. and Boettcher S., *Phys. Rev. Lett.*, **77** (1996) 111.
[27] Olson C. J. *et al.*, *Phys. Rev. B*, **56** (1997) 6175.